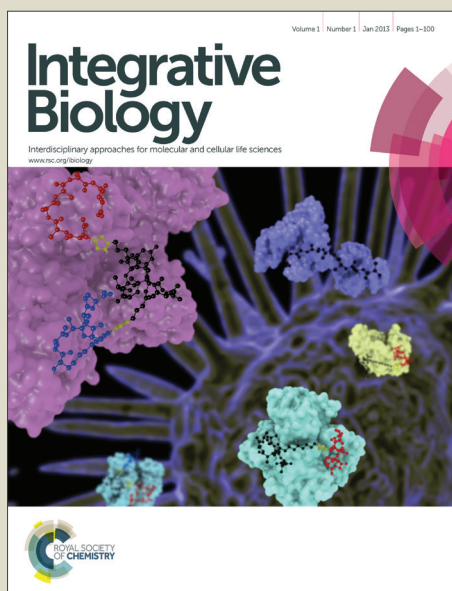


Integrative Biology

Accepted Manuscript



This is an *Accepted Manuscript*, which has been through the Royal Society of Chemistry peer review process and has been accepted for publication.

Accepted Manuscripts are published online shortly after acceptance, before technical editing, formatting and proof reading. Using this free service, authors can make their results available to the community, in citable form, before we publish the edited article. We will replace this *Accepted Manuscript* with the edited and formatted *Advance Article* as soon as it is available.

You can find more information about *Accepted Manuscripts* in the [Information for Authors](#).

Please note that technical editing may introduce minor changes to the text and/or graphics, which may alter content. The journal's standard [Terms & Conditions](#) and the [Ethical guidelines](#) still apply. In no event shall the Royal Society of Chemistry be held responsible for any errors or omissions in this *Accepted Manuscript* or any consequences arising from the use of any information it contains.

SCHOLARONE™
Manuscripts

Integrative Biology Accepted Manuscript

1 **Functional analysis of single cells identifies a rare subset of**
2 **circulating tumor cells with malignant traits**

3
4 Xiaosai Yao^{1,2}, Atish D. Choudhury^{4,5,6}, Yvonne J. Yamanaka^{1,2},
5 Viktor A. Adalsteinsson^{1,3,6}, Todd M. Gierahn¹, Christina A. Williamson⁷, Carla R. Lamb
6⁸, Mary-Ellen Taplin^{4,5}, Mari Nakabayashi⁴, Matthew Chabot⁴, Tiantian Li⁴, Gwo-Shu
7 M. Lee⁴, Jesse S. Boehm⁶, Philip W. Kantoff^{4,5}, William C. Hahn^{4,5,6},
8 K. Dane Wittrup^{1,2,3 *}, and J. Christopher Love^{1,3,6 *}
9
10

11 ¹ David H. Koch Institute for Integrative Cancer Research, ² Department of Biological
12 Engineering, ³ Department of Chemical Engineering, Massachusetts Institute of
13 Technology, Cambridge, Massachusetts 02139, USA
14

15 ⁴ Dana-Farber Cancer Institute, Boston, Massachusetts 02215
16

17 ⁵ Harvard Medical School, Boston, Massachusetts 02115
18

19 ⁶ Broad Institute of Harvard and MIT, Cambridge, Massachusetts 02142
20

21 ⁷ Department of Thoracic and Cardiovascular Surgery, ⁸ Department of Interventional
22 Pulmonology, Lahey Hospital and Medical Center, Massachusetts 01803
23
24

25 ***Corresponding authors**

26 J. Christopher Love
27 500 Main St. 76-253, Cambridge, MA 02139
28 Phone: 617-324-2300
29 Fax: 617-258-5042
30 Email: clove@mit.edu
31

32 K. Dane Wittrup
33 500 Main St. 76-261D, Cambridge, MA 02139
34 Phone: 617-253-4578
35 Fax: 617-253-1954
36 Email: wittrup@mit.edu
37

38 The authors declare no conflicts of interest.

39 **Total word count:** 4800

40 **Number of figures:** 5

41 **Key words:** circulating tumor cells, metastasis, heterogeneity, single-cell

1 **Abstract**

2 Ample evidence supports genetic and functional heterogeneity in primary tumors, but it
3 remains unclear whether circulating tumor cells (CTCs) also exhibit the same
4 hierarchical organization. We examined the functional diversity of viable, single CTCs
5 using an array of subnanoliter wells (nanowells). The compartmentalization of single
6 cells by nanowells allowed clonal comparison and mapping of heterogeneity of single
7 cells or preformed clusters of cells. By measuring the short-term viability, invasiveness
8 and secretory profiles of individual CTCs, it was evident that only a rare subset of CTCs
9 possessed malignant traits indicative of metastatic potential in late-stage, progressing
10 metastatic castration-resistant prostate cancer (mCRPC) patients. These CTCs were
11 resistant to anoikis after being in the circulation, were invasive in their epithelial state, or
12 secreted proteases capable of cleaving peptide substrates. Every CTC observed,
13 however, did not exhibit such metastatic potential, suggesting that enumeration of CTCs
14 alone may be insufficient to understand metastasis or stratify patients.

15

16 **Insight, Innovation and Integration**

17 Circulating tumor cells (CTCs) may mediate the hematogenous dissemination of cancer
18 and initiate metastasis. However, their paucity at 1 cell/ml blood makes direct functional
19 characterization challenging. We exploited spatially-addressable arrays of nanowells to
20 measure short-term viability, invasiveness and secretory profiles of individual CTCs. We
21 found that individual CTCs exhibit heterogeneous behavior, with only a rare subset of
22 them being anoikis-resistant or invasive. This nanowell-based approach allowed
23 compartmentalization and spatiotemporal tracking of individual cells or clusters, and
24 thus enabled us to gain new insight into the largely dormant and selectively malignant
25 population of CTCs.

26

1 Introduction

2 Circulating tumor cells (CTCs) mobilize from primary tumors or metastases and
3 transit through the bloodstream. They are of fundamental interest because a
4 subpopulation of CTCs may initiate metastasis and mediate the hematogenous
5 dissemination of cancer ¹. The recent successful engraftment of CTCs in xenograft
6 models provided convincing evidence that metastasis-initiating cells exist amongst
7 CTCs ^{2, 3}. Because these assays used pooled CTCs, however, it remains unclear if
8 every CTC contributes equally to tumor formation, or if a founder population possesses
9 enhanced tumorigenic potential and gives rise to metastatic colonies ⁴. Identifying the
10 cells, or a subpopulation of cells, most capable of establishing overt metastasis may be
11 one key to designing effective therapies, especially if such cells are rare and can evade
12 conventional chemotherapies ⁵ and remain dormant for a number of years in the form of
13 minimal residual disease ⁴.

14 To adequately resolve the fine variance within a population of CTCs, it is
15 important to both isolate rare CTCs and interrogate each CTC individually, preferably in
16 a high-throughput fashion. Current assays, however, either require pooled CTCs ^{2, 3},
17 obscuring any heterogeneous differences in cellular behaviors among cells, or fail to
18 preserve cell viability. Existing single-cell assays are mainly confined to enumeration ⁶,
19 intracellular staining ⁷, genotyping ⁸, and gene expression⁹. Because these assays
20 require fixation or lysis, it has not been possible to evaluate several important
21 characteristics of live CTCs, including their viability over time and their propensity to
22 invade or secrete soluble factors. These functional phenotypes could provide potentially
23 useful indicators of the metastatic potential of tumor cells ¹⁰⁻¹².

24 Here we developed a process using arrays of subnanoliter wells (nanowells) ¹³ to
25 isolate and characterize single, viable CTCs from whole blood, thereby exploring the
26 functional diversity amongst CTCs. This approach enabled us to perform spatiotemporal
27 tracking of CTCs and identify a rare subset of CTCs that exhibited malignant traits
28 indicative of metastatic potential.

29

1 **Materials and Methods**

2 **Patient recruitment**

3 The patient cohort used in this study was generated from the Prostate Clinical Research
4 Information System (CRIS) at the Dana-Farber Cancer Institute. The CRIS system
5 consists of data-entry software, a central data repository, collection of patient data
6 including comprehensive follow-up of all patients, and tightly integrated security
7 measures as previously described¹⁴. All patients provided written informed consent to
8 allow the collection of tissue and blood and the analysis of clinical and genetic data for
9 research purposes. Patients with metastatic castration-resistant prostate cancer were
10 identified for this trial based on 1) progression on a phase II study of abiraterone in
11 combination with dutasteride or 2) Prostate-specific Antigen (PSA) >20 ng/ml to enrich
12 for patients likely to have detectable CTCs. Patient status was assigned by changes in
13 serum PSA levels, with progression at the time of blood collection defined as a PSA
14 increase of >5% per 30 days. Refer to **Supplementary Table 1** for patient information.
15 Blood was drawn into EDTA tubes and processed within 4 hr. Whole blood from healthy
16 donors was purchased from Research Blood Components.

17

18 **Fabrication of arrays of nanowells**

19 A silicon master¹⁵ was microfabricated (Stanford foundry) and mounted in a metal mold.
20 Poly(dimethylsiloxane) (PDMS) (Dow Corning) (10:1 ratio of base to catalyst) was
21 injected through a port into the silicon mold, cured at 80°C for 4 hr, and then removed to
22 produce an array containing 84,672 cubic wells (65 μm). Before use, the PDMS array
23 was oxygen plasma treated for 2 min and immediately submerged in PBS to preserve
24 the hydrophilicity rendered by the plasma treatment. The array was then blocked in
25 serum-containing media for 15 min before cells were loaded.

26

27 **Enrichment of CTCs**

28 Negative selection was performed using either the EasySep or RosetteSep CD45
29 depletion kit (StemCell Technologies). With the EasySep kit, 45 ml of red blood cell lysis
30 buffer (Biolegend) was added to 5 ml of whole blood and the mixture was incubated at
31 room temperature until the red blood cells were completely lysed (15 – 20 min). Blood

1 was washed once with wash buffer (2% Fetal Bovine Serum (FBS), 1% Bovine Serum
2 Antigen (BSA), 5 mM Ethylenediaminetetraacetic acid (EDTA) in Phosphate Buffered
3 Saline (PBS)). CD45 depletion was performed with the EasySep human CD45 depletion
4 kit according to the manufacturer's instructions. The remaining cells were suspended in
5 approximately 200 μ l wash buffer and were directly deposited onto the PDMS nanowells
6 and allowed to settle for 5 min. With the RosetteSep kit, 250 μ l antibody cocktail was
7 incubated with 5 ml of whole blood for 20 min. The blood was then diluted with PBS at a
8 1:1 ratio and layered onto Ficoll-Paque Plus (GE Healthcare) in a SepMate tube
9 (StemCell Technologies) and centrifuged at 800x g for 10 min. The upper layer
10 containing the serum and buffy coat was removed and washed twice. Further red blood
11 cell lysis was sometimes necessary to remove residual red blood cells.

12

13 **Staining and microscopy**

14 Cells were either stained directly on the array of nanowells in a tube for 1 hr at room
15 temperature with EpCAM and a cocktail of lineage markers for leukocytes including
16 CD3, CD16, CD20, CD38 and CD45 (refer to the list of antibodies used in
17 **Supplementary Table 2**). For viability assays, the cells were rinsed with PBS and
18 stained with Calcein AM violet (Molecular Probes) and Annexin V FITC (BD
19 Pharmingen) in Annexin V binding buffer (BD Pharmingen) for 10 min at room
20 temperature.

21

22 The stamps were imaged with an epifluorescence microscope (Zeiss) with filter wheels
23 at the following wavelengths: Calcein AM violet (Ex: 390 nm, Em: 440/40 nm), FITC (Ex:
24 488 nm, Em: 525/36 nm), PerCP-eFluor710 (Ex: 488 nm, Em: 716/40nm), PE/CY7 (Ex:
25 570 nm, Em: 809/81 nm)

26

27 Compensation was performed with beads that were precoated with anti-Fc antibodies
28 (Bangs Laboratories). Each antibody was incubated with the beads and imaged in all
29 the fluorescent channels. The percentage of bleed over was computed by plotting the
30 fluorescence intensity of the signal channel versus the intensity of all other channels

1 individually. The slope of the linear plot gave the percentage bleed over of the signal
2 channel into the second channel.

3
4 Cells were identified with Enumerator, a custom image analysis software developed in
5 house. For each nanowell array, we generated a list of cell information including the
6 well IDs, cell size and fluorescent intensities. The text file was converted into a FlowJo-
7 readable text format ¹⁶. Gating and cell statistics were analyzed in Flowjo (Treestar).

8
9 **Proliferation assay**

10 CTCs were cultured directly in the nanowells. C4-2 cells were obtained from ATCC.
11 Matrigel (1 ml; BD Biosciences) was added directly onto the nanowells and allowed to
12 solidify for 1 hr at room temperature. Cells were maintained in a growth medium that
13 was previously reported to enhance the proliferation of epithelial cells ¹⁷. The growth
14 medium consisted of 3:1 Ham's F-12 Nutrient Mixture-Dulbecco's modified Eagle's
15 medium (Cellgro), 5% FBS (Sigma-Aldrich), 0.4 µg/ml hydrocortisone (Sigma-Aldrich),
16 insulin (5 µg/ml) - transferrin (5 µg/ml) - sodium selenite (5 ng/ml) supplement (Roche),
17 8.4 ng/ml cholera toxin (Sigma-Aldrich), 100 U/ml Penicillin-Streptomycin (Cellgro), 10
18 ng/ml epidermal growth factor (Life Technologies), 24 µg/ml adenine (Sigma-Aldrich),
19 10 µM Y-27632 (Enzo Life Sciences) and 1 pM 5α-Androstan-17β-ol-3-one (Sigma-
20 Aldrich). In addition to the growth conditions described above, we applied a second
21 culture condition that has previously been used to grow intestinal stem cells and primary
22 prostate cancer cells ¹⁸. The growth medium consisted of 3:1 Ham's F-12 Nutrient
23 Mixture-Dulbecco's modified Eagle's medium (Cellgro), 1x N2 supplements (Life
24 Technologies), 1x B-27 supplements (Life Technologies), 1 mM N-acetylcysteine
25 (Sigma-Aldrich), 1 µg/ml R-spondin (Life Technologies), 100 ng/ml Noggin (Life
26 Technologies), 50 ng/ml epidermal growth factor (Life Technologies), 100 U/ml
27 penicillin-streptomycin (Cellgro), 10 µM Rho-kinase (ROCK) inhibitor (Y-27632) (Enzo
28 Life Sciences) and 1 pM 5α-Androstan-17β-ol-3-one (Sigma-Aldrich). There was,
29 however, no significant difference in the percentage of CTC survival between the two
30 culture conditions.

1 The cells were relabeled with antibodies against EpCAM, CD3, CD16, CD20, CD38 and
 2 CD45 and calcein AM, and then imaged every three days. Viability was defined by
 3 positive calcein AM and EpCAM staining as well as intact cell morphology in the bright
 4 field.

5
 6 The predicted probability of the viability of a cluster was estimated based on the viability
 7 of a single cell. A cluster was considered viable if it contained at least one viable cell.
 8 The viabilities of clusters containing different numbers of cells were weighted by the
 9 frequencies of each cluster according to the following formula:

$$P_{cluster, viable} = \frac{1}{N} \sum_{i=2}^{i_{max}} i \times n_i (1 - (1 - P_{single, viable})^i)$$

10 where N = total number of cells found in clusters, i = number of cells found in a cluster
 11 (ranging from 2 to i_{max}), n_i = number of clusters containing i cells and $P_{single, viable}$ =
 12 viability of single cells.

14 **Invasion assay**

15 After cell loading, 1 ml of Matrigel was pipetted directly onto the nanowell arrays and
 16 allowed to solidify for 1 hr at room temperature. Cells embedded in Matrigel were
 17 stained with antibodies (1:200) for 2 hr at 37 °C before imaging. The array was then
 18 imaged every three days. EpCAM⁺ cells were identified and tracked by their positive
 19 EpCAM staining. The coordinates of the centroid of the individual cells or cell clusters
 20 and of their wells were read in AxioVision (Zeiss). The relative coordinates of the cells to
 21 the wells were calculated as:

$$cell_{rel} = (rel_x, rel_y) = (x_{cell} - x_{well}, y_{cell} - y_{well})$$

23
 24 The distance that the cells had moved from their initial position was calculated as:

$$distance = \sqrt{(rel_x^{day 1} - rel_x^{day n})^2 + (rel_y^{day 1} - rel_y^{day n})^2}$$

26

1 **Microengraving**

2 Microengraving was performed as previously described ¹⁹. Poly-lysine-coated glass
3 slides were coated with 1 µg of capture antibody in 80 µl sodium borate buffer (pH 9) for
4 1 hr at room temperature or 4°C overnight and then blocked in PBS + 1% BSA for 30
5 min. The cell-loaded array of nanowells was rinsed with basal media containing 0.04%
6 human serum. Human IgGs in the serum were used to mark the position of each well;
7 every well should be positive for human IgG because anti-human IgG capture and
8 detection antibodies were included in the panel of antibodies. The antibody-coated
9 glass slide was then sealed on top of the nanowells in a hybridization clamp for 4 hr at
10 37°C. The slide was then blocked with 5% milk + 0.5% TWEEN-20 + PBS (blocking
11 buffer) for 15 min and incubated with 0.3 µg fluorescently conjugated detection
12 antibodies in 150 µl of blocking buffer for 45 min at room temperature. The dried slide
13 was scanned with a GenePix 4400A scanner (Molecular Devices). The scanned image
14 was analyzed with Matlab programs developed in house, Crossword and Matchbox.
15 The IgG background channel was used to identify the position of each well. A positive
16 event was defined as a well that 1) had 50% of its pixels 2 standard deviations above
17 the mean intensity of the background and 2) $3 \leq \text{signal-to-noise ratio (SNR)} \leq 12$. Each
18 positive event was further manually inspected for potential artifacts.

19
20 The calibration curve for determining rates of secreted PSA was constructed by spotting
21 1 µl of diluted PSA detection antibody (1 µg/µl) (5000x – 10,000,000x dilution) on a
22 poly-lysine slide. The slide was dried under vacuum for 5 min and then scanned using
23 the same settings as the clinical samples. The median intensity was quantified using
24 GenePix Pro 6.0 (Molecular Devices).

25

26 **Proteolytic assay with Fluorescence Resonance Energy Transfer (FRET)-based** 27 **peptides**

28 Whole blood from a prostate cancer patient was first enriched for CTCs using the
29 RosetteSep CD45 depletion kit. The cells were then loaded into the nanowells and
30 stained with Calcein AM Violet, EpCAM and lineage antibody cocktail for 1 hr. Next, 500
31 µl of 5 µM FRET polypeptides (BioZyme) mixture was added to the array of nanowells.

1 A glass slide was sealed over the array using a hybridization clamp for 3 hr in a
2 humidifier chamber. The array of nanowells was then imaged with the microscope
3 using the FITC channel (Ex: 488 nm, Em: 525/36 nm) for the FRET peptides. The
4 peptides are substrates of Matrix Metalloproteinases (MMPs) 1, 2, 8, 9, 10, 12, 13 and
5 14 and A Disintegrin and Metalloproteinases (ADAMs) 8, 10, 17 as described previously
6 ²⁰. The sequences of the peptides are shown in **Supplementary Table 3**.

7
8 After the initial time point, the arrays of nanowells containing CTCs were placed in the
9 lower chamber of a 0.2 μm transwell petri dish (Corning). C4-2 cells (1×10^4 cells,
10 ATCC) and MG-63 cells (1×10^6 cells, ATCC) were seeded on top of the transwell. The
11 0.2 μm transwell allowed secreted factors from C4-2 cells and MG-63 cells to diffuse to
12 the CTCs in the lower chamber. The cells were maintained in growth medium as
13 described in the proliferation assay for one week, at which point the proteolytic activity
14 was measured again.

15
16
17

1 **Results**

2 **Isolation of circulating tumor cells with arrays of subnanoliter wells**

3 In order to resolve the variance between individual CTC, we developed a system
4 to characterize single cells in a high-throughput manner. Our PDMS array comprises
5 84,762 cubic wells of 275 pL each (65 μm x 65 μm x 65 μm). CTCs were enriched from
6 whole blood by negative selection against CD45 and loaded onto the array to settle into
7 the nanowells by limiting serial dilution (**Fig. 1a**). Because CTCs are rare, the loading
8 biased the occupancy of each well to single CTCs or preformed clusters, allowing
9 comparisons among individual CTCs.

10 To interrogate all the cells, we imaged the entire array and obtained the surface
11 fluorescence and position of every cell using a custom-designed image processing
12 software (on-chip cytometry). In addition to surface fluorescence, we were also
13 interested in measuring the secretion of individual cells. We placed glass slides
14 functionalized with capture antibodies in contact with the nanowells to capture soluble
15 factors secreted by cells in the individual wells in a process known as microengraving¹³.
16 Because the unique well ID retains the spatial information of each cell, we can visually
17 inspect rare cells with their images, track the same cells over time and map secretion
18 events back to the respective cells (**Fig. 1b**). Using this approach, we were able to
19 make three types of measurements on viable CTCs isolated from patients with prostate
20 cancer: (1) immediate and short-term viability of CTCs, (2) invasive potential of CTCs,
21 and (3) secretion of soluble factors (**Fig. 1a**).

22 We validated the performance of our method using spiked tumor cell lines. We
23 estimated the yield of our process to be 30% using C4-2 prostate tumor cells and HT29
24 colon tumor cells (**Fig. 1c**). The depletion of CD45⁺ cells was the dominant source of
25 loss (**Supplementary Fig. 1**). The process maintained the viability of the isolated tumor
26 cells (95% \pm 10% for HT29 cells and 90% \pm 7% for C4-2 cells). Therefore, viability of
27 CTCs lower than 90% is a likely result of previous apoptotic events, rather than death
28 induced from processing.

29

30 **A subset of circulating tumor cells is viable at the time of isolation**

1 Previously reported methods have not distinguished among viable and dead
2 CTCs from blood samples. Therefore, we determined the viability of primary CTCs
3 isolated from the blood of prostate cancer patients. We applied a combination of live
4 (calcein AM⁺) and apoptotic (Annexin V⁺) markers in addition to lineage markers
5 (EpCAM⁺CD45⁻). The non-fluorescent Calcein AM is hydrolyzed to a fluorescent form by
6 intracellular esterases in live cells, while Annexin V binds to phosphatidylserine on
7 apoptotic cells. Using imaging cytometry, we analyzed CTCs isolated from the blood of
8 prostate cancer patients and categorized them as either fully viable (Calcein AM⁺/
9 Annexin V⁻), apoptotic (Calcein AM⁺/ Annexin V⁺), dead (Calcein AM⁻/ Annexin V⁺), or
10 disintegrated (Calcein AM⁻/ Annexin V⁻) (**Fig. 2a**).

11 Our results showed that a significant proportion of CTCs were already dead after
12 isolation. The range of viable CTCs observed in 18 prostate cancer patients was 0 –
13 314 cells per 5 ml of blood (mean = 25, median = 0) (**Fig 2b**, bottom panel). Viable
14 EpCAM⁺ cells were completely absent in 5 ml of blood of 60% of mCRPC patients.
15 Since most CTC enumeration methods count the aggregate number of viable, apoptotic
16 and dead cells (**Fig 2b**, top panel), previous analyses may have overestimated the
17 abundance of biologically active CTCs.

18

19 **The majority of circulating tumor cells undergo rapid cell death**

20 A subset of CTCs may represent “in transit” tumor cells with metastatic potential,
21 but the rate-limiting step of metastasis is thought to be colonization at the distant site²¹.
22 We therefore sought to determine whether viable CTCs isolated from blood maintained
23 their viability and/or possessed proliferative potential.

24 We tracked the viability (**Fig. 3a**) and the surface area (**Fig. 3b**) as a proxy for
25 proliferation (cells in a cluster fused and could not be accurately counted after a week in
26 culture) in 125 CTCs from patient ID2 and 48 spiked C4-2 prostate cancer cells for 16
27 days in Matrigel. Tracking was possible because CTCs maintained expression of
28 EpCAM and other cell types started to die as early as day 4. Both the CTCs and C4-2
29 cells had clusters of cells and single cells. In the case of C4-2 cells, a subset of cells
30 experienced substantial growth (**Fig. 3b**), forming colonies from single cells or clusters
31 (**Fig. 3c**). In contrast, none of the primary CTCs exhibited sustained proliferation. Most

1 surviving CTCs spread out after becoming adherent to the Matrigel but remained
2 dormant throughout the 16 days of culture (**Fig. 3b, c**), suggesting that CTCs have a
3 low *in vitro* clonogenic potential compared with prostate cancer cell lines. The absence
4 of any proliferative cells might be a result of their low abundance or the inability of our *in*
5 *vitro* system to mimic the important stromal factors found *in vivo*. We also cultured the
6 CTCs using different conditions (see Methods) and with co-culture of fibroblasts, but
7 none of these culture conditions resulted in proliferation.

8 We observed that the overall viability of single cells declined at a faster rate than
9 did cell clusters for both CTCs and C4-2 cells (**Fig. 3a**). We asked whether being in a
10 cluster imparted enhanced survival to cells. Since we considered the entire cluster to be
11 viable if at least one cell remained alive, we needed to correct for the higher number of
12 cells found in a cluster (see Methods for formula). We compared the observed and
13 predicted viability of clusters extrapolated from single cells (**Fig. 3a**) and found that
14 clusters of CTCs did not show enhanced survival but clusters of C4-2 cells had an
15 increased survival rate compared with single cells.

16 We cultured CTCs from 10 more patients in Matrigel in nanowells for up to 7
17 days (**Fig. 3d**). Similar to that of patient ID2, most CTCs underwent cell death, but a
18 small number of cells remained viable after a week of culture in Matrigel (**Fig. 3d**). We
19 did not observe outgrowth of CTCs in samples without any starting viable CTCs (in case
20 some CTCs could upregulate their EpCAM expression once becoming established in
21 culture). The two patients (ID1 and ID2) with the highest number of persistent CTCs
22 were deceased within six months of their blood draws. Therefore, it is possible that the
23 presence of large numbers of persistent CTCs indicate an aggressive clinical disease
24 and poor patient outcome. These persistent cells appeared resistant to anoikis after
25 being in the circulation and thus may have the potential to colonize when growth
26 conditions become favorable.

27

28 **A subset of circulating tumor cells is invasive**

29 In addition to clonogenic potential, the invasiveness of tumor cells also correlates
30 with metastatic potential. When we cultured CTCs from patient ID2, we noticed that
31 even though CTCs did not proliferate, they could invade through the Matrigel layer.

1 Therefore, we quantified the invasiveness of individual CTCs from patients ID1 and ID2.
2 Both patients had single cells and cell clusters in their blood samples (**Supplementary**
3 **Fig. 2**), although clusters from patient ID1 comprised only doublets whereas clusters
4 from patient ID2 ranged from two to nine cells.

5 Using each CTC's original well as a reference point, we monitored cell movement
6 by recording the coordinates of the cells' centroids over time (**Fig. 4a, Supplementary**
7 **Fig. 3**). Clusters from patient ID1 did not exhibit enhanced invasive behavior relative to
8 single cells (**Fig. 4b**). On the other hand, cell clusters from patient ID2 exhibited a
9 greater range of migration compared with single cells (**Fig. 4b**). Single cells and cell
10 clusters of patient ID2 also differed significantly in their invasive behavior, ranging from
11 no movement to over 100 μm in two weeks.

12

13 **A subset of circulating tumor cells secretes PSA and proteolytic enzymes.**

14 One key advantage of the nanowells is the ability to use them to detect secreted
15 factors from single cells with high sensitivity and specificity. We used microengraving (4
16 hr) to detect the secretion of prostate specific antigen (PSA) from CTCs. While EpCAM
17 staining can only ascribe the histological classification of a cell to be epithelial, secretion
18 of a tissue-specific protein such as PSA can further reveal the origin of CTCs. Using a
19 signal-to-noise ratio (SNR) of 3 to 12, we could distinguish spiked prostate cancer cells
20 (C4-2 and LNCaP) from blood cells and HT29 colon tumor cells with 100% specificity
21 (**Supplementary Fig. 4**). We sought to determine whether CTCs in the blood produce
22 PSA. We detected secretion of PSA by CTCs from prostate cancer patients (**Fig. 5a**),
23 but surprisingly, only from a very small subset of cells. For example, only 2/31 CTCs of
24 patient ID3 secreted PSA above the threshold. Furthermore, the number of PSA-
25 secreting events did not correlate with serum PSA levels. The rate of detectable PSA
26 secretion by CTCs was low, ranging from 0.05-0.2 pg/hr/cell (**Supplementary Fig. 5**),
27 implying that PSA secreted by CTCs is a negligible source of total serum PSA (typically
28 in the ng/ml range). This result also suggests that CTCs make up only a small fraction
29 of the total tumor burden in a patient if serum PSA correlates with tumor volume²². We
30 also used microengraving to measure five other secreted factors—MMP9, CXCL1, 5, 8
31 and VEGF, but we did not detect these factors from CTCs.

1 In addition to directly measuring secreted PSA, we also measured the activity of
2 enzymes secreted into the wells by observing the cleavage of their substrates. We
3 incubated enriched CTCs with FRET-based polypeptide protease substrates²⁰
4 (moderately specific for matrix metalloproteinases (MMPs) and A disintegrin and
5 metalloproteinases (ADAMs)) in the nanowells. Only a small proportion of CTCs
6 cleaved the substrates immediately after isolation (**Fig. 5b**). To mimic the paracrine
7 interactions in the bone microenvironment since prostate cancer cells have a tendency
8 to metastasize to the bone tissue, we cultured the CTCs with conditioned media from
9 MG63 osteosarcoma cells and C4-2 prostate cancer cells. After a week in culture, two
10 of the five surviving CTCs cleaved the peptides to a greater degree than did freshly
11 isolated CTCs, resulting in an increase in the fluorescent signal within the well (**Fig. 5d**).
12 These results indicate that CTCs can secrete proteolytic enzymes necessary to break
13 down extracellular matrix.

14

15

1 Discussion

2 Heterogeneity among CTCs adds complexity to the understanding of cancer
3 metastasis. We demonstrated that CTCs found in mCRPC patients exhibit functional
4 heterogeneity in terms of viability, invasiveness and proteolytic activity, with as few as
5 2% of the total viable CTCs possessing malignant traits in progressing patients. For
6 example, patient ID3 had 117 viable CTCs at the time of isolation but only 2/117
7 remained viable on day 7. In a separate experiment, only 2/86 CTCs of the same
8 patient secreted proteolytic enzymes. The rarity of malignant CTCs agrees with two
9 pieces of evidence supporting metastatic inefficiency. First, the low engraftment rate of
10 CTCs in an immunocompromised mouse model, and the requirement for at least 10^3
11 CTCs to initiate tumor formation, suggest that metastatic initiating cells (MICs) comprise
12 a rare fraction of total CTCs². Second, the discrepancy between the number of CTCs (0
13 – 23,618 cells per 7.5 ml of peripheral blood⁶) and the number of metastases (1-13
14 lesions per patient²³) implies that the majority of the shed tumor cells are incapable of
15 progressing to overt metastases.

16 One advantage of our nanowell-based platform relative to conventional flow
17 cytometry is that each cell is documented with an optical image, allowing us to visually
18 inspect the intactness, morphology, and spatial distributions of labeled proteins for each
19 cell. This feature is important for verifying rare events when the number of false
20 positives can be similar to that for true positives. Our platform can also be coupled with
21 a robotic manipulator to recover single cells for genotyping.

22 Here we have provided two additional pieces of evidence to account for the low
23 frequency of tumorigenic CTCs: 1) significant apoptosis during and after circulation and
24 2) dormancy of CTCs. By preserving the viability of isolated CTCs, we quantified the
25 distribution of viable and dead cells. The relatively high percentage of apoptotic cells we
26 saw agree with previous studies that detected a significant number of apoptotic CTCs
27 by Terminal deoxynucleotidyl transferase dUTP nick end labeling (TUNEL) assay²⁴ or
28 caspase cleavage at cytokeratin 18^{25, 26}. Because these previous studies used an
29 intracellular marker, however, they could not directly quantify the presence of viable
30 cells. Our data indicated that only 22% of the patients have ≥ 1 viable cells in 1 ml of
31 blood after isolation. The majority of these surviving cells continued to undergo rapid

1 cell death after leaving the circulation, and only a few cells could persist in Matrigel
2 culture for over two weeks.

3 Secondly, we found that these viable CTCs are in a quiescent state. The
4 observation that these CTCs are non-proliferative may seem surprising initially but
5 corroborates an earlier study that failed to detect any Ki-67 staining in the CTCs of 47
6 breast cancer patients ²⁷. A separate genetic analysis of CTCs also showed that
7 compared with established cell lines, CTCs had a quiescent phenotype, with a
8 decreased expression of growth factors such as *VEGFA*, *MET*, *ESR1*, *EGFR*, and
9 *HER2* and the cell cycle genes downstream of these growth factors including *MYC*,
10 *ATF3*, *TERT*, *RAC1*, *FOXA1*, *RRM1*, *CCNB1*, and *BIRC5* ²⁸. It is important to realize
11 that the proliferative potential of CTCs found in patients differs significantly from that of
12 cell lines. Conventional chemotherapy is ineffective in eliminating single dormant cells in
13 the bone marrow of cancer patients ²⁹ because these dormant cells evade drugs that
14 target proliferating cells. These dormant cells may have the potential to restart their
15 proliferative program after a number of years as minimal residual disease ¹. Accordingly,
16 the presence of dormant disseminated tumor cells correlates with a worse prognosis
17 and a higher rate of relapse ³⁰⁻³².

18 We demonstrated for the first time that clusters of CTCs could exhibit invasive
19 phenotypic behaviors while retaining their expression of EpCAM, an epithelial marker.
20 This collective cell invasion, in which multicellular units invade while maintaining their
21 cell-cell junction molecules, was thought to be the predominate form of invasion in
22 highly differentiated tumors such as epithelial prostate cancer ^{33, 34}. While experimental
23 evidence has demonstrated the importance of epithelial-mesenchymal transition for cell
24 invasion to occur, and has thus raised the question whether CTCs expressing EpCAM,
25 an epithelial marker, can be invasive. This result suggests that the loss of epithelial
26 markers is not a requirement for invasion to occur. Furthermore, consistent with our
27 observation that the invasive CTCs were quiescent, an earlier study identified primary
28 tumor cells in the invasive margin of ductal carcinoma to be invasive yet dormant.
29 These cells were enriched for pro-migratory and anti-proliferative genes relative to
30 intratumoral cells ³⁵. An *in vitro* model using tumor cell lines encapsulated in 3D

1 collagen matrices also demonstrated that tumor cells could be highly invasive and
2 dormant, but knockdown of p27 could reverse this dormancy³⁵.

3 In this study, we focused our efforts on examining EpCAM⁺ cells, but we did not
4 exclude the possibility that EpCAM⁻ cells exist and may equally constitute a major
5 source of tumorigenic CTCs³. We observed the presence of persistent EpCAM⁻ cells
6 even though they are rare. Together with additional markers, such as PMSA, we may
7 further explore whether these cells are potentially prostate in origin.

8 In conclusion, interrogating the functional behavior of individual CTCs allowed us
9 to demonstrate that CTCs from the same patient differ significantly in their viability,
10 invasiveness and secretory profiles. We identified a rare subset among isolated CTCs
11 with phenotypes consistent with more efficient metastasis in mCRPC patients. Cells in
12 this subset can resist apoptosis, invasive, or they can secrete proteolytic enzymes. If
13 and when these cells escape cell arrest, they may cause tumor recurrence. Therefore,
14 therapy to target this subset of cells³⁶ may be necessary to eliminate minimal residual
15 disease. Future studies incorporating a sufficiently powered cohort of patients and new
16 CTC markers (e.g., PSMA) could potentially provide further insights into how functional
17 behavior of CTCs affects patient outcome. The functional assessment of individual
18 CTCs was accomplished by our spatially-addressable array of nanowells that allowed
19 compartmentalization and spatiotemporal tracking of individual cells or clusters. The
20 nanowell-based approach can be further expanded to retrieve the individual cells to
21 investigate whether this functional diversity may arise from genetic or epigenetic factors,
22 thus helping us to better understand cancer dissemination and design therapies to
23 counter it.

24

25 **Acknowledgements**

26 J.C.L. is a Camille Dreyfus Teacher-Scholar. This work was supported by Janssen
27 Pharmaceuticals. This work was also supported in part by the Koch Institute Support
28 (core) Grant P30-CA14051 from the National Cancer Institute. X.Y. was supported by a
29 fellowship from A*STAR, Singapore. A.D.C is supported by the Prostate Cancer
30 Foundation Young Investigator Award and the DoD Physician Scientist Training Award.
31 V.A.A. was supported in part by a graduate fellowship from the National Science

1 Foundation. The authors dedicate this paper to the memory of Officer Sean Collier, for
2 his caring service to the MIT community and for his sacrifice.

3

4 **Author contributions**

5 X.Y. A.D.C, Y.J.Y, K.D.W and J.C.L conceived the experiments. X.Y., Y.J.Y., V.A.A.,
6 and T.M.G. developed and performed nanowell-based assays, and analyzed single-cell
7 data. A.D.C., C.A.W., C.R.L., M.T., M.N., G.M.L., T.L, M.S.C., J.S.B. and P.W.K, wrote
8 the IRB protocol, recruited patients and provided clinical specimens. X.Y., K.D.W., and
9 J.C.L. wrote the manuscript.

10 **References**

- 11 1. Pantel K, Alix-Panabieres C, Riethdorf S. Cancer micrometastases. *Nature*
12 *Reviews Clinical Oncology* 2009; 6:339-51.
- 13 2. Baccelli I, Schneeweiss A, Riethdorf S, Stenzinger A, Schillert A, Vogel V, et al.
14 Identification of a population of blood circulating tumor cells from breast cancer patients
15 that initiates metastasis in a xenograft assay. *Nature Biotechnology* 2013; 31:539-U143.
- 16 3. Zhang LX, Ridgway LD, Wetzel MD, Ngo J, Yin W, Kumar D, et al. The
17 Identification and Characterization of Breast Cancer CTCs Competent for Brain
18 Metastasis. *Science Translational Medicine* 2013; 5.
- 19 4. Pantel K, Brakenhoff RH, Brandt B. Detection, clinical relevance and specific
20 biological properties of disseminating tumour cells. *Nature Reviews Cancer* 2008;
21 8:329-40.
- 22 5. Muller V, Stahmann N, Riethdorf S, Rau T, Zabel T, Goetz A, et al. Circulating
23 tumor cells in breast cancer: correlation to bone marrow micrometastases,
24 heterogeneous response to systemic therapy and low proliferative activity. *Clin Cancer*
25 *Res* 2005; 11:3678-85.
- 26 6. Allard WJ, Matera J, Miller MC, Repollet M, Connelly MC, Rao C, et al. Tumor
27 cells circulate in the peripheral blood of all major carcinomas but not in healthy subjects
28 or patients with nonmalignant diseases. *Clinical Cancer Research* 2004; 10:6897-904.
- 29 7. Stott SL, Lee RJ, Nagrath S, Yu M, Miyamoto DT, Ulkus L, et al. Isolation and
30 Characterization of Circulating Tumor Cells from Patients with Localized and Metastatic
31 Prostate Cancer. *Science Translational Medicine* 2010; 2.
- 32 8. Maheswaran S, Sequist LV, Nagrath S, Ulkus L, Brannigan B, Collura CV, et al.
33 Detection of mutations in EGFR in circulating lung-cancer cells. *New England Journal of*
34 *Medicine* 2008; 359:366-77.
- 35 9. Ramskold D, Luo SJ, Wang YC, Li R, Deng QL, Faridani OR, et al. Full-length
36 mRNA-Seq from single-cell levels of RNA and individual circulating tumor cells. *Nature*
37 *Biotechnology* 2012; 30:777-82.
- 38 10. Li L. Correlation of Growth Capacity of Human Tumor Cells in Hard Agarose With
39 Their In Vivo Proliferative Capacity at Specific Metastatic Sites. *J Natl Cancer Inst* 1989;
40 81: 1406-12.

- 1 11. Inoue K, Slaton JW, Eve BY, Kim SJ, Perrotte P, Balbay MD, et al. Interleukin 8
2 expression regulates tumorigenicity and metastases in androgen-independent prostate
3 cancer. *Clinical Cancer Research* 2000; 6:2104-19.
- 4 12. Repesh LA. A new in vitro assay for quantitating tumor cell invasion. *Invasion*
5 *Metastasis* 1989; 9:192-208.
- 6 13. Love JC, Ronan JL, Grotenbreg GM, van der Veen AG, Ploegh HL. A
7 microengraving method for rapid selection of single cells producing antigen-specific
8 antibodies. *Nat Biotechnol* 2006; 24:703-7.
- 9 14. Oh WK, Hayes J, Evan C, Manola J, George DJ, Waldron H, et al. Development
10 of an integrated prostate cancer research information system. *Clin Genitourin Cancer*
11 2006; 5:61-6.
- 12 15. Ogunniyi AO, Story CM, Papa E, Guillen E, Love JC. Screening individual
13 hybridomas by microengraving to discover monoclonal antibodies. *Nat Protoc* 2009;
14 4:767-82.
- 15 16. Simm M.
- 16 17. Liu XF, Ory V, Chapman S, Yuan H, Albanese C, Kallakury B, et al. ROCK
17 Inhibitor and Feeder Cells Induce the Conditional Reprogramming of Epithelial Cells.
18 *American Journal of Pathology* 2012; 180:599-607.
- 19 18. Sato T, Clevers H. Primary mouse small intestinal epithelial cell cultures.
20 *Methods Mol Biol*; 945:319-28.
- 21 19. Han Q, Bradshaw EM, Nilsson B, Hafler DA, Love JC. Multidimensional analysis
22 of the frequencies and rates of cytokine secretion from single cells by quantitative
23 microengraving. *Lab on a Chip* 2010; 10:1391-400.
- 24 20. Miller MA, Barkal L, Jeng K, Herrlich A, Moss M, Griffith LG, et al. Proteolytic
25 Activity Matrix Analysis (PrAMA) for simultaneous determination of multiple protease
26 activities. *Integr Biol (Camb)*; 3:422-38.
- 27 21. Luzzi KJ, MacDonald IC, Schmidt EE, Kerkvliet N, Morris VL, Chambers AF, et al.
28 Multistep nature of metastatic inefficiency: dormancy of solitary cells after successful
29 extravasation and limited survival of early micrometastases. *Am J Pathol* 1998;
30 153:865-73.
- 31 22. Carvalhal GF, Daudi SN, Kan D, Mondo D, Roehl KA, Loeb S, et al. Correlation
32 Between Serum Prostate-specific Antigen and Cancer Volume in Prostate Glands of
33 Different Sizes. *Urology* 2010; 76:1072-6.
- 34 23. Klein CA. Parallel progression of primary tumours and metastases. *Nature*
35 *Reviews Cancer* 2009; 9:302-12.
- 36 24. Mehes G, Witt A, Kubista E, Ambros PF. Circulating breast cancer cells are
37 frequently apoptotic. *American Journal of Pathology* 2001; 159:17-20.
- 38 25. Rossi E, Fassan M, Aieta M, Zilio F, Celadin R, Borin M, et al. Dynamic changes
39 of live/apoptotic circulating tumour cells as predictive marker of response to Sunitinib in
40 metastatic renal cancer. *British Journal of Cancer* 2012; 107:1286-94.
- 41 26. Larson CJ, Moreno JG, Pienta KJ, Gross S, Repollet M, O'Hara SM, et al.
42 Apoptosis of circulating tumor cells in prostate cancer patients. *Cytometry Part A* 2004;
43 62A:46-53.
- 44 27. Muller V, Stahmann N, Riethdorf S, Rau T, Zabel T, Goetz A, et al. Circulating
45 tumor cells in breast cancer: Correlation to bone marrow micrometastases,

- 1 heterogeneous response to systemic therapy and low proliferative activity. *Clinical*
2 *Cancer Research* 2005; 11:3678-85.
- 3 28. Powell AA, Talasz AH, Zhang HY, Coram MA, Reddy A, Deng G, et al. Single
4 Cell Profiling of Circulating Tumor Cells: Transcriptional Heterogeneity and Diversity
5 from Breast Cancer Cell Lines. *Plos One* 2012; 7.
- 6 29. Murray NP, Reyes E, Tapia P, Badinez L, Orellana N, Fuentealba C, et al.
7 Redefining micrometastasis in prostate cancer - a comparison of circulating prostate
8 cells, bone marrow disseminated tumor cells and micrometastasis: Implications in
9 determining local or systemic treatment for biochemical failure after radical
10 prostatectomy. *International Journal of Molecular Medicine* 2012; 30:896-904.
- 11 30. Alix-Panabieres C, Vendrell JP, Pelle O, Rebillard X, Riethdorf S, Muller V, et al.
12 Detection and characterization of putative metastatic precursor cells in cancer patients.
13 *Clinical Chemistry* 2007; 53:537-9.
- 14 31. Aguirre-Ghiso JA. Models, mechanisms and clinical evidence for cancer
15 dormancy. *Nat Rev Cancer* 2007; 7:834-46.
- 16 32. Wiedswang G, Borgen E, Karesen R, Qvist H, Janbu J, Kvalheim G, et al.
17 Isolated tumor cells in bone marrow three years after diagnosis in disease-free breast
18 cancer patients predict unfavorable clinical outcome. *Clin Cancer Res* 2004; 10:5342-8.
- 19 33. Friedl P, Wolf K. Tumour-cell invasion and migration: diversity and escape
20 mechanisms. *Nat Rev Cancer* 2003; 3:362-74.
- 21 34. Friedl P, Locker J, Sahai E, Segall JE. Classifying collective cancer cell invasion.
22 *Nature Cell Biology* 2012; 14:777-83.
- 23 35. Raviraj V, Zhang H, Chien HY, Cole L, Thompson EW, Soon L. Dormant but
24 migratory tumour cells in desmoplastic stroma of invasive ductal carcinomas. *Clinical &*
25 *Experimental Metastasis* 2012; 29:273-92.
- 26 36. Yu Z, Schmaltz RM, Bozeman TC, Paul R, Rishel MJ, Tsosie KS, et al. Selective
27 tumor cell targeting by the disaccharide moiety of bleomycin. *Journal of the American*
28 *Chemical Society* 2013; 135:2883-6.
- 29

1 **Figure 1: Functional measurements of viability, invasion and secretory profiles of**
2 **CTCs using arrays of nanowells**

- 3 a) Scheme for the enrichment and functional characterization of CTCs using
4 nanowells for 1) viability, 2) invasion, or 3) secretion of soluble factors.
5 b) Scatter plot (left) is generated from on-chip imaging cytometry of 50 C4-2 cells
6 spiked into 5 ml of whole blood. Image analysis software extracted the
7 fluorescence intensities of all the cells on the array, and plotted as a scatter plot
8 similar to that used in flow cytometry. A single cell can be mapped back to its
9 original image (middle) or secretion event determined by microengraving (right)
10 based on its unique well ID.
11 c) Efficiency of recovery of tumor cells from whole blood is about 30% using spiked
12 HT29 and C4-2 cells.
13

14 **Figure 2: Viability of CTCs at the time of isolation**

- 15 a) Assessment of the viability of CTCs using on-chip cytometry measurements of
16 apoptosis (Annexin V) and viability (Calcein AM). Gating of EpCAM⁺ cells (left)
17 yields a population of EpCAM⁺CD45⁻ cells that are scored for both Annexin V and
18 Calcein AM (middle) to classify viable cells (1), apoptotic cells (2), dead cells (3)
19 and disintegrated cells (4). Representative phase contrast and epifluorescence
20 micrographs (right) are shown for each classified state.
21 b) Bargraphs of the number of CTCs by classified state of viability. The numbers of
22 total intact EpCAM⁺ cells (top), Calcein AM⁺/EpCAM⁺ cells (middle) and Calcein
23 AM⁺/AnnexinV/EpCAM⁺ cells (bottom) are shown for 18 prostate cancer patients
24 (red) and 6 healthy donors (black).
25

26 **Figure 3: Short-term viability of CTCs is low compared to that of C4-2 cells**

- 27 a) Viability of single cells and clusters of cells. Left: viability of single C4-2 cells
28 (black line, n = 34), clusters of C4-2 cells (red solid line, n = 32) and predicted
29 viability of clusters of C4-2 cells (red dashed line). Right: viability of single CTCs
30 (black line, n = 23), clusters of CTCs (red solid line, n = 9) and predicted viability
31 of clusters of CTCs (red, dashed line) from patient ID2.
32 b) Fold changes in the surface area of single cells or clusters of C4-2 cells or CTCs
33 from patient ID2 over 16 days.
34 c) Representative micrographs of the proliferation of a single C4-2 cell, a cluster of
35 5 C4-2 cells, a single CTC from patient ID2, and a cluster of 3 CTCs from patient
36 ID2 in Matrigel cultured over 16 days. EpCAM staining is in magenta.
37 d) Bargraph of the number of viable CTCs as a function of time in culture. Only
38 4/10 patients had persistent viable CTCs after one week in Matrigel culture in the
39 nanowells (red bar).
40

41 **Figure 4: CTCs migrate and secrete PSA and proteolytic enzymes**

- 42 a) Micrographs (top) of an EpCAM⁺ cluster of CTCs isolated from patient ID2 (red)
43 in Matrigel and the corresponding plot of the movement of the centroid of the
44 cluster as a function of time (bottom).
45 b) Heat maps of the cumulative distance moved by the CTCs isolated from two
46 patients. Each row represents a single cell or a cell cluster.

1

2 Figure 5: CTCs secrete PSA and proteolytic enzymes

- 3 a) Scatter plot of the signal-to-noise ratio of secreted PSA measured by
4 microengraving for 5 prostate cancer patients, 6 healthy donors and 2 prostate
5 cancer cell lines. Each dot indicates one measured well. Micrographs of the
6 secreted PSA (green) and control measure (human IgG; red) are shown for a subset
7 of events. The red dashed line (SNR = 5) indicates the threshold set to discriminate
8 between healthy donors and prostate cancer patients. Red arrows denote PSA
9 positive events.
- 10 b) Histogram of the proteolytic activity of CTCs as measured by the cleavage of FRET-
11 based polypeptide substrates immediately after isolation (gray) or after one week in
12 culture (red). The micrograph shows one example of a positive signal (green)
13 generated by an EpCAM⁺ cell (magenta) after 7 days.
14

Figure 1

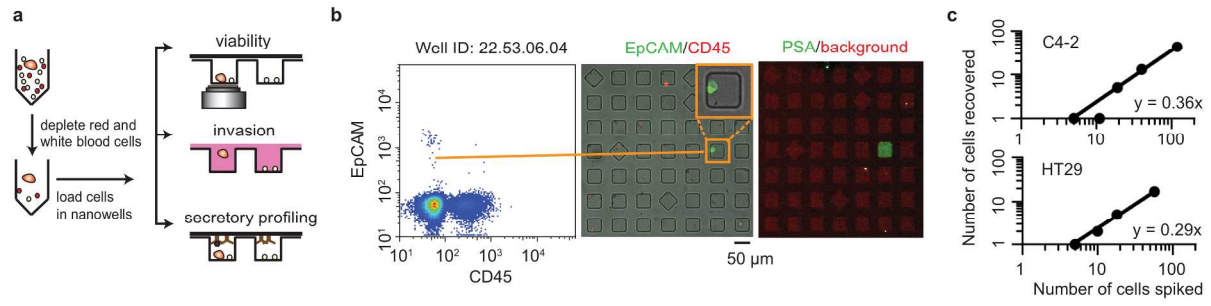


Figure 2

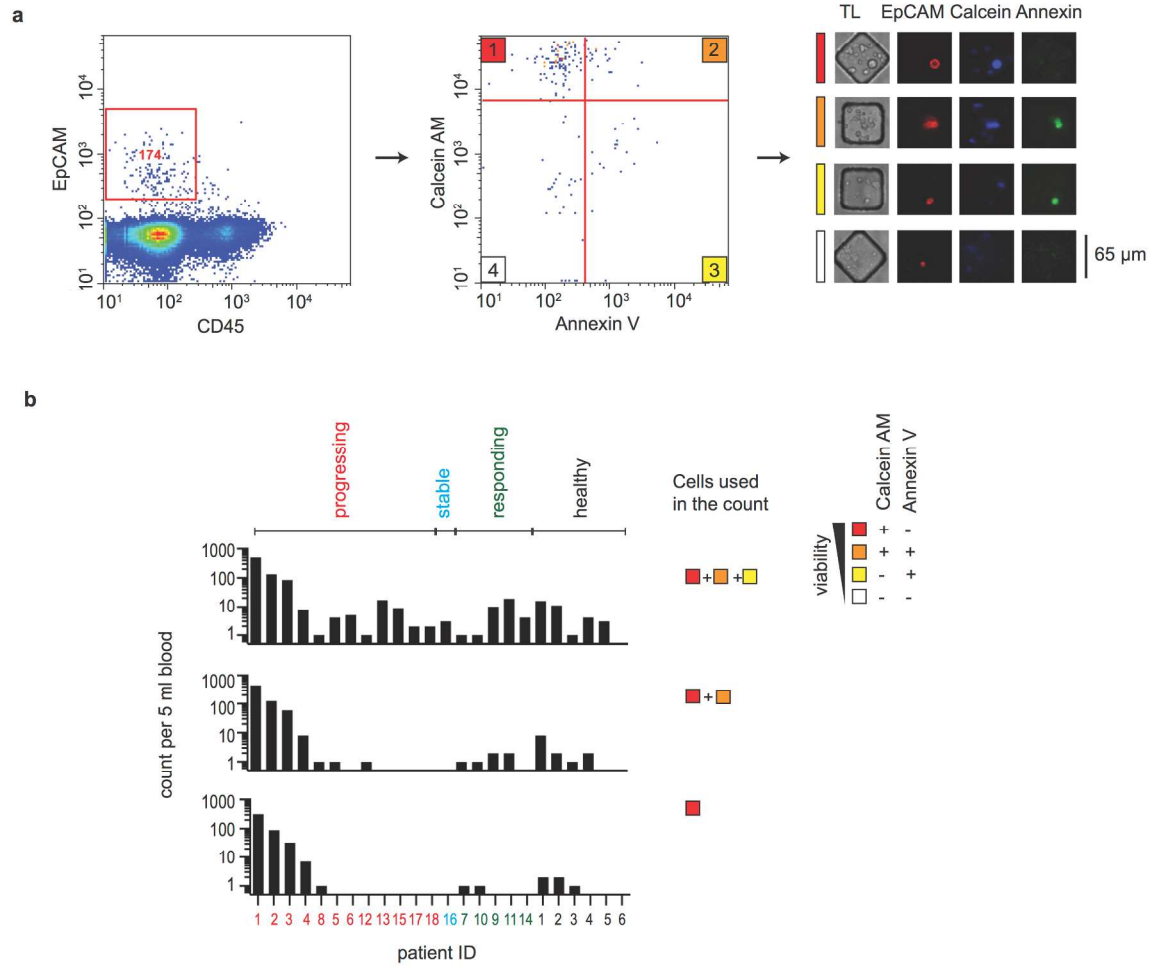


Figure 3

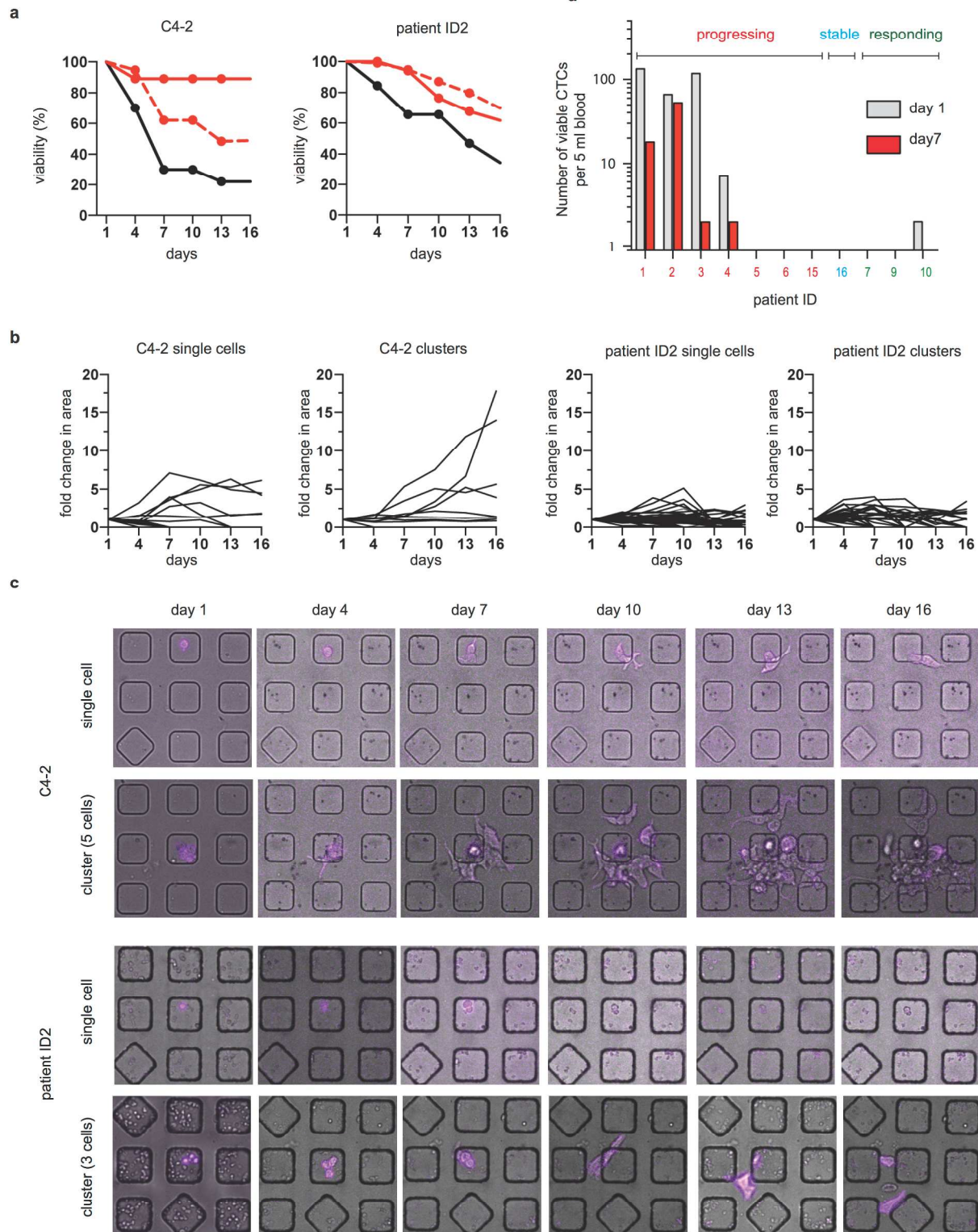


Figure 4

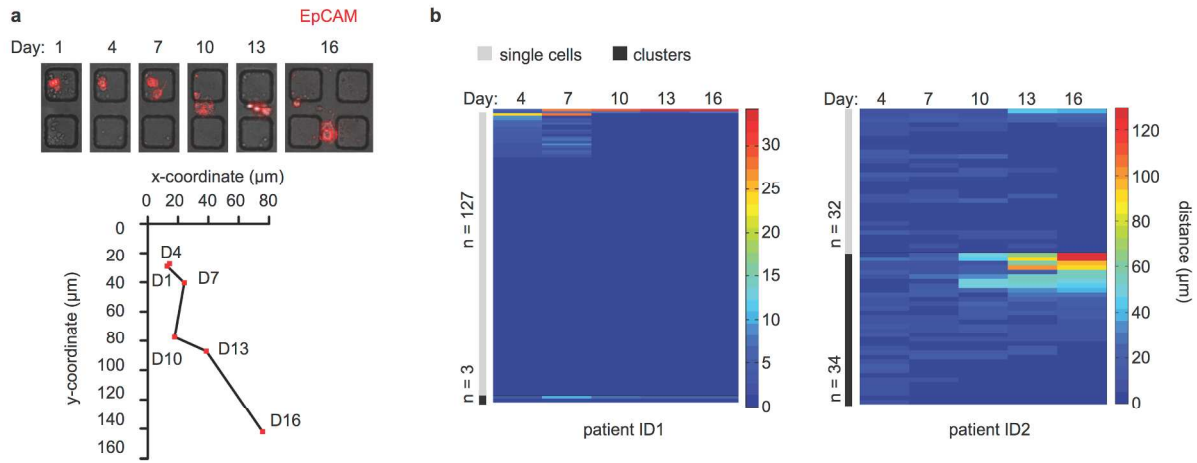
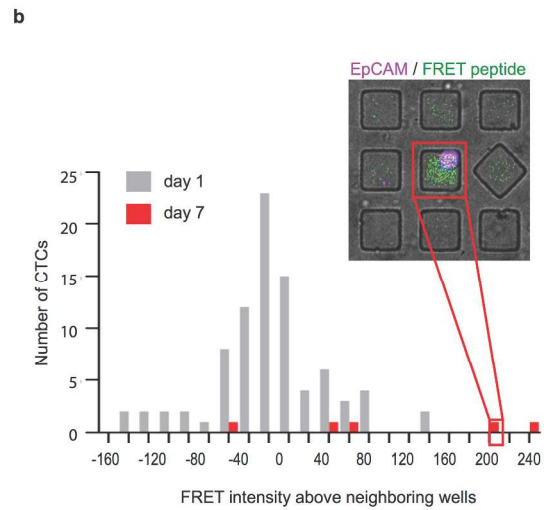
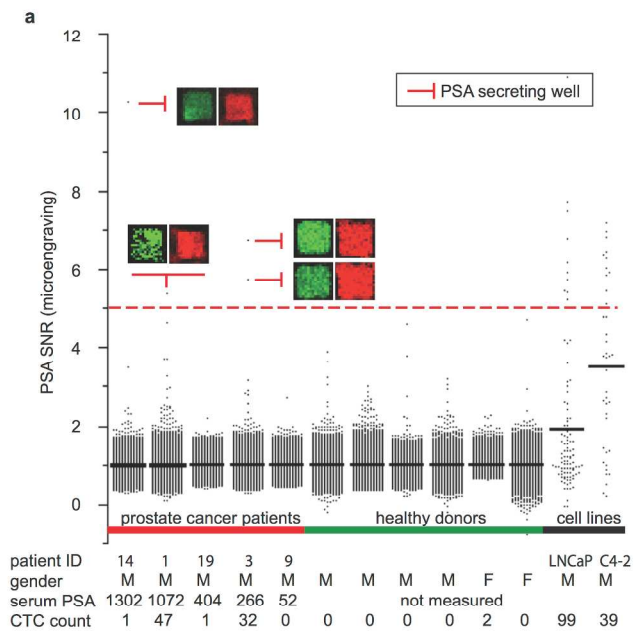


Figure 5



We measured the viability, invasiveness and secretion of single circulating tumor cells on an array of nanowells.

